nature structural & molecular biology

Crystal structures of the PsbS protein essential for photoprotection in plants

Minrui Fan[1,2], Mei Li[1], Zhenfeng Liu[1], Peng Cao[1], Xiaowei Pan[1], Hongmei Zhang[1], Xuelin Zhao[1], Jiping Zhang[1] & Wenrui Chang[1]

The photosystem II protein PsbS has an essential role in qE-type nonphotochemical quenching, which protects plants from photodamage under excess light conditions. qE is initiated by activation of PsbS by low pH, but the mechanism of PsbS action remains elusive. Here we report the low-pH crystal structures of PsbS from spinach in its free form and in complex with the qE inhibitor *N*,*N*′-dicyclohexylcarbodiimide (DCCD), revealing that PsbS adopts a unique folding pattern, and, unlike other members of the light-harvesting-complex superfamily, it is a noncanonical pigment-binding protein. Structural and biochemical evidence shows that both active and inactive PsbS form homodimers in the thylakoid membranes, and DCCD binding disrupts the lumenal intermolecular hydrogen bonds of the active PsbS dimer. Activation of PsbS by low pH during qE may involve a conformational change associated with altered lumenal intermolecular interactions of the PsbS dimer.

Photosynthesis is a highly efficient and dynamically regulated biochemical process driven by sunlight. In plants, photosystem II is surrounded by light-harvesting complexes (LHCs) which include the major trimeric LHCII and three minor monomeric LHCs named CP29, CP26 and CP24 (ref. 1). Light energy is absorbed by chlorophylls and carotenoids bound to the LHCs and is then transferred to the reaction centers, where charge separation occurs. Under excess light or other environmental stresses, plants often absorb more light energy than they can use for carbon dioxide assimilation, and this excess absorption can result in oxidative damage and even cell death[2,3]. To limit potential photo-oxidative damage, plants have evolved a very efficient protective mechanism called energy-dependent quenching (qE-type nonphotochemical quenching), through which the excess absorbed light energy can be safely dissipated as heat[4–6]. qE occurs on a time scale of seconds to minutes, and it has an important physiological role for plants grown in fields, where light intensity rapidly fluctuates[7].

qE is generally believed to depend on four key elements[5,6,8,9]: the transthylakoid change in pH (ΔpH, in which the lumenal pH of 5.5–5.8 under excess light conditions is approximately two units lower than the stromal pH of 7.5–8.0 (ref. 10)), the xanthophyll zeaxanthin[11], the LHCs[12–14] and the PsbS protein of PSII[15]. PsbS is essential for qE in plants[15–17], and its expression level is a determinant of qE capacity[16,18,19]. Despite extensive research efforts on PsbS, its mechanism of action in qE has remained an enigma[6,8,17,20]. PsbS was previously shown to bind pigments[21–23] and has been suggested to be the direct quenching site[15,24]; however, recent evidence has indicated that PsbS is not a pigment-binding protein and that it acts as a pH-sensitive trigger of qE[25,26]. Under high-light conditions, the pH of thylakoid lumen decreases to below 6.0 (ref. 10). PsbS can sense this acidification of the lumenal side and become activated[24]. The pH-sensing residues of PsbS are two lumen-exposed glutamates, to which the carboxyl-modifying reagent DCCD can bind and inhibit qE[27]. PsbS may experience a conformational change upon activation, and previous studies have suggested that low lumenal pH activates PsbS by inducing its dimer-to-monomer transition during qE[28]. Studies have also shown that in the absence of PsbS, qE can be induced on a much slower timescale (hours) *in vivo*[29] or can be restored by enhanced ΔpH (with a lumenal pH of 3.9) *in vitro*[30], thus suggesting that the role of PsbS is to allow qE to turn on rapidly at physiological lumenal pH. Nevertheless, exactly how PsbS functions in qE remains to be elucidated.

To shed light on the mechanism of PsbS action in qE, we determined the crystal structures of spinach PsbS and its complex with DCCD. Our structural and biochemical analyses unravel a unique folding pattern of PsbS and provide insights into how PsbS is activated by low pH and inhibited by DCCD.

RESULTS

Overall structure

Obtaining sufficient quantities of stable PsbS protein from native sources has been a major challenge that has limited crystallographic study of PsbS. Through careful optimization of the biochemical procedures (Online Methods), we purified the PsbS protein from spinach (**Supplementary Fig. 1**). The protein sample was green, and our pigment analysis revealed that it contained primarily chlorophyll *a* (Chl *a*) and a small amount of chlorophyll *b* (Chl *b*) (**Supplementary Fig. 2**). This result is consistent with previous reports showing that PsbS purified by isoelectric focusing contains bound

[1]National Laboratory of Biomacromolecules, Institute of Biophysics, Chinese Academy of Sciences, Beijing, China. [2]University of Chinese Academy of Sciences, Beijing, China. Correspondence should be addressed to W.C. (wrchang@sun5.ibp.ac.cn) or M.L. (meili@moon.ibp.ac.cn).

Received 2 March; accepted 14 July; published online 10 August 2015; doi:10.1038/nsmb.3068

Table 1 Data collection and refinement statistics

	Hg derivative	Native 1	Native 2	DCCD modified
Data collection				
Space group	$P2_12_12_1$	$P2_12_12_1$	$P2_12_12_1$	$P2_12_12_1$
Cell dimensions				
a, *b*, *c* (Å)	72.0, 78.2, 93.0	72.1, 78.4, 93.2	72.0, 77.5, 93.2	71.7, 77.7, 93.2
α, β, γ (°)	90.0, 90.0, 90.0	90.0, 90.0, 90.0	90.0, 90.0, 90.0	90.0, 90.0, 90.0
Resolution (Å)	50–3.10	50–3.10	50–2.35	50–2.70
	(3.21–3.10)	(3.21–3.10)	(2.43–2.35)	(2.80–2.70)
R_{merge}	0.118 (0.549)	0.104 (0.412)	0.079 (0.515)	0.103 (0.587)
$I / \sigma I$	31.4 (5.1)	41.2 (9.4)	19.1 (4.2)	15.0 (3.8)
Completeness (%)	100 (100)	100 (100)	99.4 (100)	99.7 (100)
Redundancy	13.8 (14.2)	13.8 (14.4)	5.8 (5.8)	5.1 (5.1)
Refinement				
Resolution (Å)			29.80–2.35	39.06–2.70
No. reflections			22,232	14,771
R_{work} / R_{free}			0.230 / 0.266	0.232 / 0.284
No. atoms				
Protein			2,552	2,516
Ligand / ion			149 / 1	116 / 7
Water			43	3
B factors				
Protein			46.3	45.3
Ligand / ion			83.7 / 37.8	58.8 / 81.1
Water			47.9	43.8
r.m.s. deviations				
Bond lengths (Å)			0.004	0.005
Bond angles (°)			0.915	0.763

Values in parentheses are for highest-resolution shell.

pigments[22,31]. We crystallized spinach PsbS at pH 5.0 and determined the low-pH crystal structures of both native and DCCD-modified PsbS at 2.35-Å and 2.7-Å resolution, respectively (**Table 1** and **Supplementary Fig. 3**).

In our structure, PsbS contains four transmembrane helices (TM1–TM4) assembled into a compact structure (**Fig. 1a**). Two long intertwined helices, TM1 and TM3, form a central supercoil and are flanked by two short helices, TM2 and TM4. The four transmembrane helices of PsbS are connected by an elongated stromal loop and two short lumenal loops. On the stromal side, the β1 strand next to TM2 forms a short antiparallel β-sheet with the β2 strand following TM4. The backbone hydrogen bonds between the two β strands contribute to the stability of the overall structure of PsbS. On the lumenal side, two amphiphilic helices, H1 and H2, are located in the lumenal loop regions.

The PsbS structure displays an internal pseudo-two-fold symmetrical relationship between its first and second half, consistently with the high sequence identity (58%) between the two halves of the protein. Interestingly, the two lumenal loops, connecting TM1 to TM2 and TM3 to TM4, adopted different conformations despite their high sequence similarity (**Fig. 1b**,**c**). The two pH-sensing glutamate residues of spinach PsbS, Glu69 and Glu173 (equivalent to Glu122 and Glu226 in *Arabidopsis*[27]), are located in the two lumenal loops (**Fig. 1a–c**).

Previous studies on the *Arabidopsis* PsbS mutants have shown that E108Q and E212Q (equivalent to Glu55 and Glu159 in spinach) severely affect the function of PsbS in qE[32]. The structure revealed that Glu55 and Glu159 anchor the two lumenal amphiphilic helices H2 and H1 to TM1 and TM3, respectively (**Fig. 1d**). Their mutations would impair the stability of the two lumenal helices as well as the overall folding of PsbS. Structure-based rationalization of the effects of other missense mutations on PsbS in the previous reports[32,33] are illustrated in **Supplementary Figure 4**.

Comparison with other LHCs

PsbS belongs to the LHC superfamily of Chl *a*– and Chl *b*–binding proteins[34–36]. It has a remarkably different overall architecture than the other LHCs with known structures (i.e., LHCII, CP29 and LHCI), which all adopt the LHCII general fold[20,37–40]. Unlike the other LHCs, PsbS consists of four rather than three transmembrane helices (**Fig. 2a**). PsbS has a core composed of the intertwined TM1 and TM3, which aligns with the central helix B–helix A supercoil of LHCII. However, both TM1 and TM3 in PsbS are shorter than helices B and A in LHCII. Moreover, the crossing angle between TM1 and TM3 of PsbS (approximately 50°) is 15° smaller than that between helices B and A in LHCII (approximately 65°) (**Fig. 2b**). On the stromal side, the short β-sheet with tight interactions found in PsbS has no counterpart in LHCII (**Fig. 2c**). On the lumenal side, both PsbS and LHCII have two amphipathic helices (H1 and H2 in PsbS; helices E and D in LHCII) at similar positions. Whereas helices H2 and D have approximately equal length, helix H1 is much shorter than helix E (**Fig. 2d**).

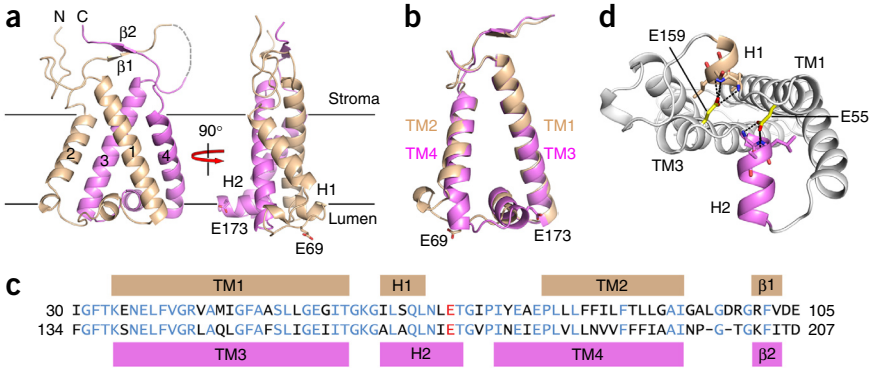

Figure 1 Overall structure of PsbS. (**a**) Ribbon representation of PsbS viewed from the membrane plane. The elongated stromal loop is partly disordered in the crystal structure, owing to its high flexibility, and is shown as a dashed line. The putative location of the thylakoid membrane is indicated. (**b**) Structural superposition of the two halves of PsbS. In **a** and **b**, the two pH-sensing glutamate residues are shown as sticks. (**c**) Sequence alignment between the two halves of PsbS, with corresponding secondary structures indicated. The two pH-sensing glutamates are highlighted in red. (**d**) The two lumenal amphiphilic helices H2 and H1 are anchored to TM1 and TM3 by Glu55 and Glu159 through hydrogen bonds (shown as black dashed lines).

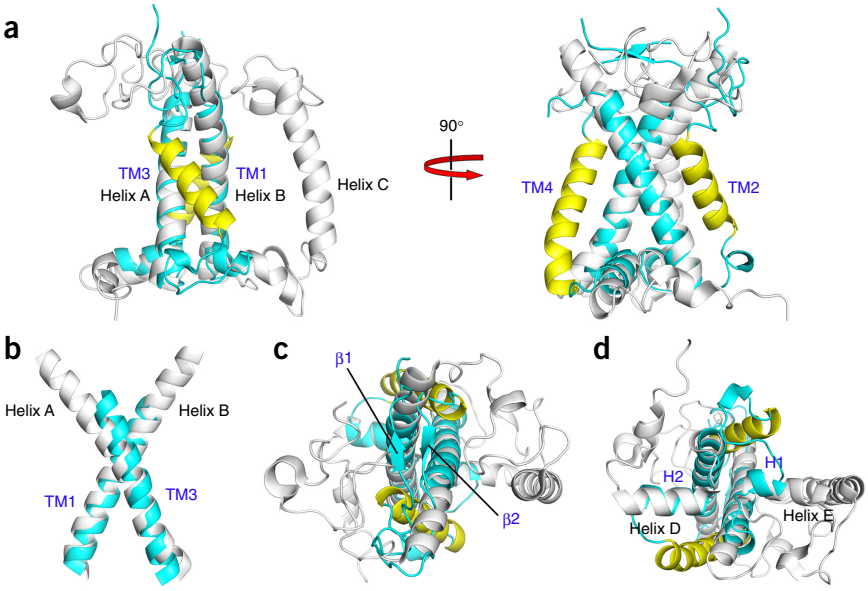

Figure 2 Structural comparison between PsbS and LHCII. (**a**) Structural superposition of PsbS and LHCII without bound pigments, viewed from the membrane plane. (**b**) Superposition of the central supercoil of PsbS and LHCII, viewed from the membrane plane. (**c**,**d**) Superpositions of PsbS and LHCII without bound pigments, viewed from the stromal side (**c**) and from the lumenal side (**d**). PsbS and LHCII are colored cyan and white, respectively. TM2 and TM4 of PsbS are colored yellow.

The most dramatic structural difference that we found between PsbS and LHCII is the relative position between TM2 (equivalent to helix C in LHCII) and the central supercoil (**Fig. 2a**). In PsbS, TM2 is located near the groove on one side of the core region, and TM4 (which has no existing counterparts in other LHCs) is located on the other side and is related to the position of TM2 through the central pseudo-two-fold axis. In LHCII, helix C is located further from the central supercoil, and a large gap between them is filled by pigment molecules.

PsbS is not an LHCII-like pigment-binding protein

The compact structure of PsbS leaves no internal void space for the formation of any pigment-binding sites. In this context, PsbS is unlike the other LHCs, which bind numerous internal pigment molecules. First, in PsbS, TM2 and the core region are too close to accommodate chlorophyll and neoxanthin molecules, which occupy the space between helix C and the core part of LHCII (**Fig. 3a**). Second, the two potential chlorophyll-ligating glutamates (Glu37 and Glu141) in PsbS, which are absolutely conserved among members of the LHC superfamily[20], cannot bind chlorophyll molecules, owing to the steric hindrance imposed by TM2 and TM4, in contrast to their counterparts in LHCII (**Fig. 3b**). Third, the locations of TM2 and TM4 in PsbS overlap partially upon superposition with those of two lutein molecules in LHCII (**Fig. 3c**). The close interactions of TM2 and TM4 with the central TM1–TM3 supercoil provide rigid support for the supercoil and thus stabilizes the overall structure of PsbS in the absence of any internal pigments; a similar role is performed by the two lutein molecules in LHCII[20,37]. Our structure now unequivocally reveals that PsbS is not a canonical pigment-binding protein (such as LHCII) and provides an explanation for previous results showing that PsbS is able to refold in the absence of pigments[26,41,42], whereas correct refolding of the other pigment-binding three-helix LHC proteins requires the presence of chlorophyll and lutein molecules[43].

Low-pH PsbS dimer

The low-pH PsbS structure showed that each asymmetric unit contained two PsbS molecules forming a homodimer related by a pseudo-two-fold axis perpendicular to the membrane (**Fig. 4a**). The TM2 and TM3 are located around the dimer interface, and TM1 and TM4 are located at the periphery of the dimer. The PsbS dimer is stabilized by extensive intermolecular interactions, including the hydrophobic interactions involving TM2 and TM3 in the transmembrane region (**Fig. 4b**); 13 hydrogen bonds, one salt bridge and one arginine-arginine pair[44] at the stromal side; and four hydrogen bonds at the lumenal side formed by the carboxyl and carbonyl oxygens of Glu173 and the backbone amide nitrogens of Ile74 and Tyr75 (**Fig. 4c**,**d** and **Supplementary Table 1**). The structure indicated that the distinct conformations adopted by the two lumenal loops of each PsbS monomer are essential for the formation of the lumenal intermolecular hydrogen bonds (**Fig. 4d**).

Interestingly, we found a large nonprotein electron density at the dimer surface, which could be interpreted as a Chl *a* molecule with reasonable fit. Concordantly, our pigment analysis of the PsbS crystals revealed that they contained mostly Chl *a* and a small amount of Chl *b* (**Supplementary Fig. 5a**,**b**). From the solubilized PsbS crystals, we calculated a stoichiometry of approximately 1.0 chlorophyll per PsbS dimer and a Chl *a*/Chl *b* ratio of 7.4. The potential Chl *a* molecule was attached at the dimer interface through hydrophobic interactions with surrounding nonpolar residues (**Supplementary Fig. 5c**). This isolated binding mode (a single Chl *a* molecule without other surrounding pigments) was consistent with the absorption and CD spectroscopic features of the purified PsbS protein (**Supplementary Fig. 5d**,**e**).

Several lines of evidence indicated that the PsbS dimer observed in the crystal structure under low-pH conditions was physiologically relevant. First, the PsbS dimer in the crystal structure contained

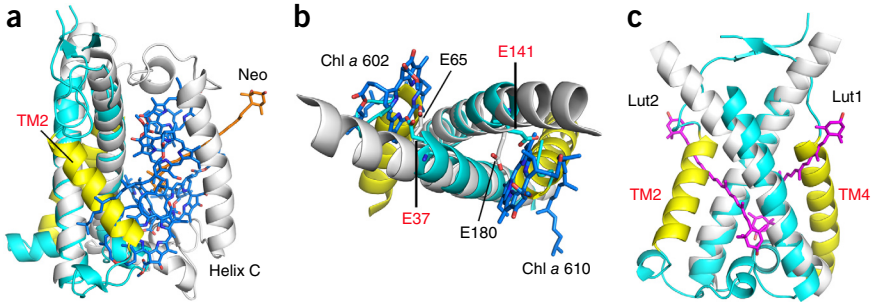

Figure 3 PsbS is not an LHCII-like pigment-binding protein. (**a**–**c**) Structural superpositions of PsbS and LHCII with bound pigments, showing the unique folding pattern of PsbS, which prevents binding of chlorophyll and carotenoid molecules. PsbS and LHCII are colored cyan and white, respectively. The chlorophyll, neoxanthin (Neo) and lutein (Lut) molecules bound to LHCII are shown as marine, orange and magenta sticks, respectively. TM2 and TM4 of PsbS are colored yellow.

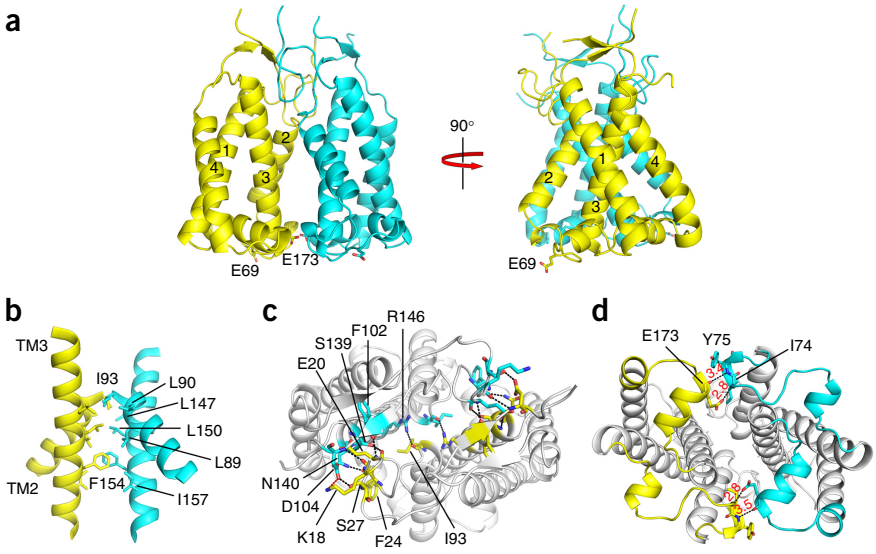

Figure 4 Structure of low-pH PsbS dimer. (**a**) Ribbon representation of PsbS dimer, with the two monomers colored yellow and cyan. (**b**) Hydrophobic interactions between TM2 and TM3 of two PsbS monomers. (**c**,**d**) Dimer-stabilizing hydrogen bonds at the stromal (**c**) and lumenal (**d**) sides.

extensive intermolecular interactions (**Fig. 4b–d**) and had a large interfacial area (over 1,600 Å^2) between the two monomers, which was predicted to be a physiological assembly by PDBePISA software[45]. Second, consistently with the crystal structure, PsbS formed dimers in the solution at pH of 5.0. We found that PsbS eluted slightly ahead of CP29 (42 kDa) from a gel-filtration column, a result consistent with the molecular weight of the PsbS dimer (44 kDa) (**Fig. 5a**). Moreover, the structure showed an intermolecular salt bridge (Lys18–Asp104) at the dimer interface (**Fig. 5b**), which was suitable for cross-linking with 1-ethyl-3-(3-dimethylaminopropyl)-carbodiimide (EDC, a zero-length cross-linker that couples carboxyl groups to primary amines with optimal efficiency at pH 4.7 to 6.0). Consistently with this, the results showed that PsbS readily formed EDC-cross-linked dimers in acidic solution (pH 3.0–5.0). There were multiple bands in each lane because un-cross-linked and cross-linked PsbS had different mobility in SDS-PAGE (in which the cross-linked PsbS was partially denatured and bound less SDS than un-cross-linked PsbS, which was fully denatured and thus migrated faster). However, when cross-linking became complete, these bands converged to two bands: cross-linked PsbS dimer and monomer (**Fig. 5c**,**d**). Third, the cross-linking experiments with low pH–incubated or high light–treated thylakoids from spinach and maize clearly revealed that the activated PsbS in the thylakoid membranes was also a dimer. In the absence of cross-linker, PsbS migrated mainly as monomers on SDS-PAGE, owing to the denaturing effect of SDS (**Fig. 5e**,**f**). We obtained similar results with high light–treated spinach chloroplasts (a more intact system that mimics *in vivo* conditions). The presence of PsbS dimer on the SDS-PAGE gel without addition of cross-linker probably resulted from incomplete denaturation of the sample (**Fig. 5g**).

It has been suggested that the transthylakoid ΔpH is important for the formation of zeaxanthin-dependent qE[46], but the maintenance of qE does not require a pH gradient; i.e., low pH alone (in the absence of a pH gradient between the stromal and lumenal sides) is sufficient to activate PsbS and maintain qE[47]. The stable dimeric structure of PsbS solved at pH 5.0 most probably represents the active form of PsbS during qE under the *in vivo* conditions. The amino acid residues that mediate PsbS dimerization are highly conserved in homologs from different plants (**Supplementary Fig. 1**), thus suggesting that the low-pH dimeric state of spinach PsbS observed in the crystal structure represents a common feature of PsbS.

The inactive state of PsbS

In addition to the dimeric form of active PsbS, the inactive form of PsbS (at neutral pH) has also been reported to be a dimer in the thylakoid membranes of maize[28]. Moreover, considering that PsbS is activated by low lumenal pH, which is sensed by two lumen-exposed glutamates of PsbS[27], and the activation process involves a putative

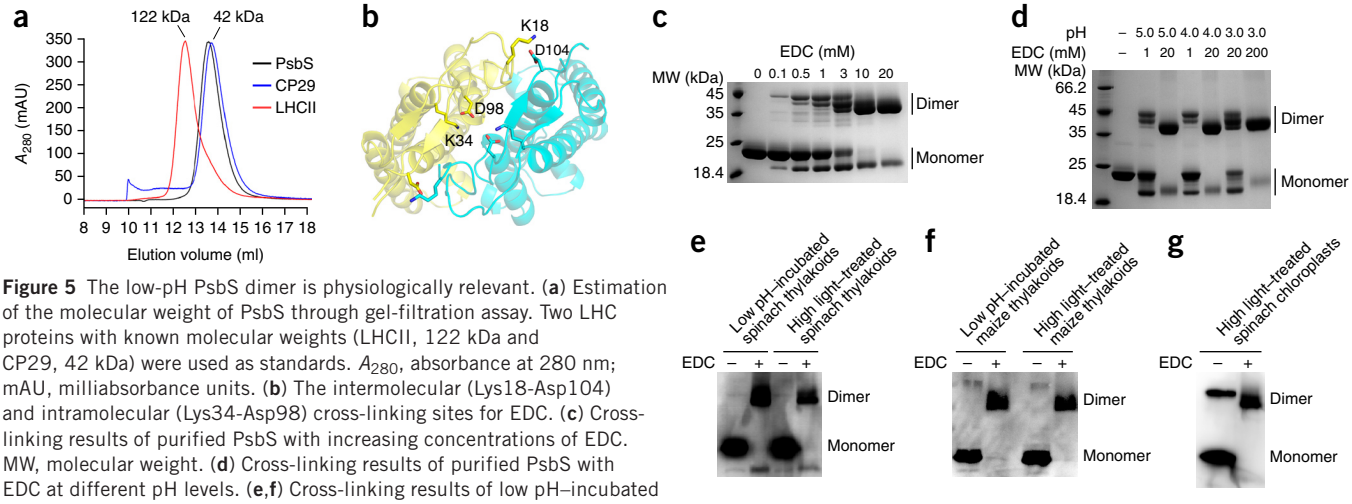

Figure 5 The low-pH PsbS dimer is physiologically relevant. (**a**) Estimation of the molecular weight of PsbS through gel-filtration assay. Two LHC proteins with known molecular weights (LHCII, 122 kDa and CP29, 42 kDa) were used as standards. A_{280}, absorbance at 280 nm; mAU, milliabsorbance units. (**b**) The intermolecular (Lys18-Asp104) and intramolecular (Lys34-Asp98) cross-linking sites for EDC. (**c**) Cross-linking results of purified PsbS with increasing concentrations of EDC. MW, molecular weight. (**d**) Cross-linking results of purified PsbS with EDC at different pH levels. (**e**,**f**) Cross-linking results of low pH–incubated or high light–treated thylakoids from spinach (**e**) and maize (**f**) with EDC. The high-molecular-weight band recognized by anti-PsbS in the thylakoids was assigned to PsbS dimer because it has the same molecular weight as that of the cross-linked purified PsbS dimer. (**g**) Cross-linking result of high light–treated spinach chloroplasts with EDC.

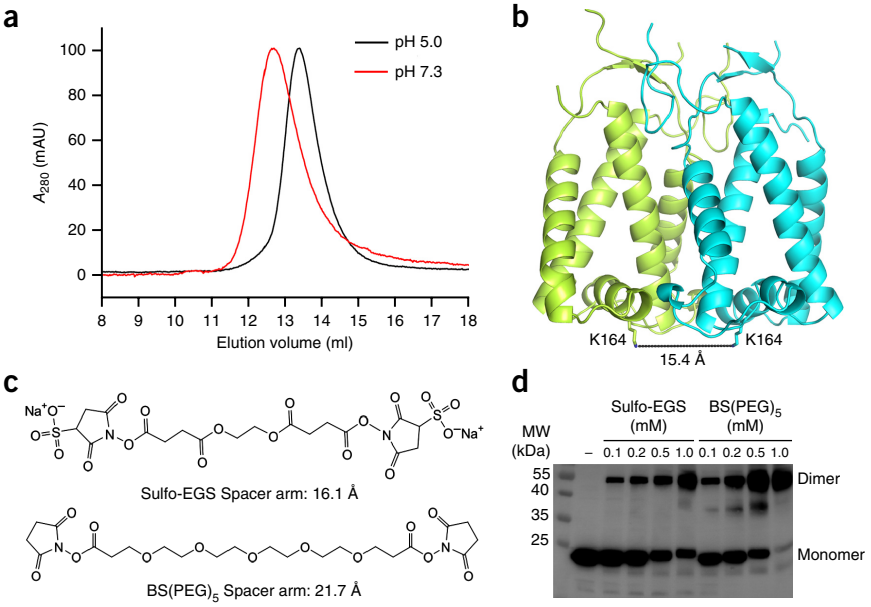

Figure 6 PsbS dimer at neutral pH. (**a**) Gel-filtration assay, showing earlier elution of PsbS at pH 7.3 than at pH 5.0. (**b**) The lumenal lysine-lysine pair at the PsbS dimer interface. (**c**) The chemical structures of the two cross-linkers, Sulfo-EGS and BS(PEG)$_5$. (**d**) Cross-linking results of dark-adapted spinach thylakoids with increasing concentrations of Sulfo-EGS or BS(PEG)$_5$ at pH 7.5.

change in its oligomeric state[28], we suggest that if the two pH-sensing residues of PsbS were mutated, PsbS could not be activated and should be locked in the oligomeric state of its inactive form even under activating conditions, i.e., low pH or high light. Our cross-linking results at pH 5.0 with low pH–incubated or high light–treated *Arabidopsis* thylakoids showed that both the pH-insensitive E122Q E226Q double mutant and the wild-type forms of PsbS existed as dimers (**Supplementary Fig. 6**). These results indicated that both inactive and active states of PsbS were dimeric, and the mutation of the two pH-sensing residues did not affect the dimeric state of PsbS.

The crystal structure of PsbS clearly showed that the pH-sensing Glu173 is important for PsbS dimerization at the lumenal side. Under neutral pH conditions, this residue should be deprotonated, thus leading to an alteration of the lumenal intermolecular hydrogen bonds. Moreover, we found that PsbS eluted earlier from a gel-filtration column at neutral pH than at acidic pH (**Fig. 6a**), a result suggesting a relatively loose conformation of the PsbS dimer under neutral pH conditions. We thus examined the differences between PsbS dimer at neutral and acidic pH. The low-pH crystal structure of PsbS revealed that at the lumenal side, there was an intermolecular lysine-lysine pair, with the residues approximately 15.4 Å apart (**Fig. 6b**). If the distance between this pair of lysine residues were to become larger upon the breakdown of the lumenal intermolecular hydrogen bonds under neutral pH conditions, the PsbS dimer would be able to be cross-linked by a cross-linker bearing a spacer arm longer than 15.4 Å. Because the purified PsbS protein was unstable and showed a tendency to precipitate at neutral pH, we performed cross-linking experiments with dark-adapted thylakoids from spinach, using two primary amine–targeted cross-linkers, sulfo-EGS and BS(PEG)$_5$, with spacer-arm lengths of 16.1 Å and 21.7 Å, respectively (**Fig. 6c**). As expected, the cross-linking results showed that PsbS readily formed sulfo-EGS– or BS(PEG)$_5$-cross-linked dimers at neutral pH (7.5) and that BS(PEG)$_5$ bearing a longer spacer arm was more effective in cross-linking (**Fig. 6d**). These results together indicated that a different conformation was adopted by the PsbS dimer at neutral pH, because the two monomers might have a larger gap at the lumenal side when the lumenal intermolecular hydrogen bonds are weakened or disrupted.

Structure of DCCD-modified PsbS

Under low-pH conditions, DCCD can bind to the pH-sensing glutamates of PsbS, causing the inhibition of qE[27]. However, it remains unclear how DCCD binds to PsbS and how exactly this interferes with the qE process. To obtain the DCCD-bound PsbS, we incubated the purified PsbS protein with DCCD at pH 5.0 and analyzed the reaction product by MS. The results showed that PsbS bound mainly one or two DCCD molecules (**Supplementary Fig. 7**), consistently with previous results[27]. The cross-linking experiment showed that the DCCD-modified PsbS protein still existed mainly as dimers in solution (**Fig. 7a**). However, our attempt to crystalize the DCCD-bound PsbS failed. We then soaked the crystal of native PsbS in DCCD-containing cryoprotectant solution and finally solved the DCCD-modified PsbS structure. The crystal structure revealed that the DCCD-modified PsbS assumes a similar dimeric form as the native PsbS. In each PsbS monomer, one molecule of DCCD is covalently bound to the carboxyl group of the pH-sensing Glu173 in the form of dicyclohexyl-*N*-acylurea (DCNU)[48] and is buried in a hydrophobic region at the dimer

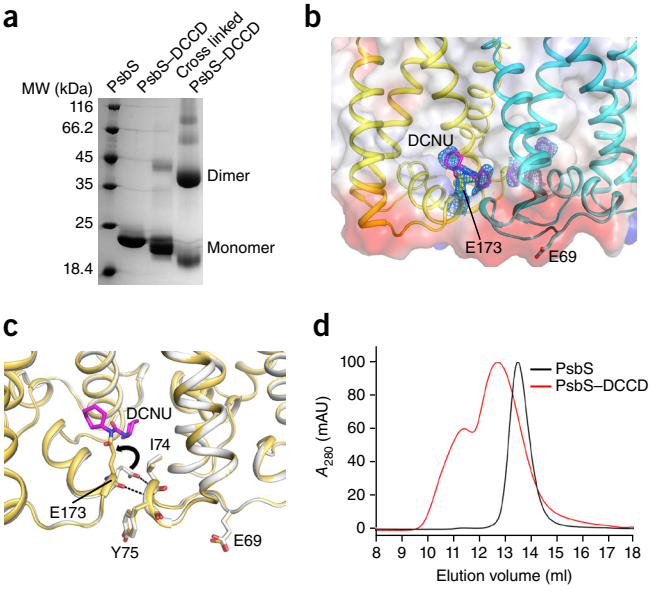

Figure 7 DCCD-modified PsbS. (**a**) Cross-linking results of DCCD-modified PsbS with EDC. (**b**) DCCD is covalently bound to the carboxyl group of Glu173 in the form of DCNU, shown with the $2F_o - F_c$ (0.8σ level) electron density. (**c**) Structural superposition of native (white) and DCCD-modified (yellow) PsbS. The DCNU molecule is shown in magenta stick representation. The rotameric switch of the Glu173 side chain upon DCCD binding is indicated by a black arrow. (**d**) Gel-filtration chromatography results showing elution of DCCD-modified PsbS ahead of native PsbS.

interface (**Fig. 7b**). Comparison between the structures of native and DCCD-modified PsbS revealed that DCCD binding induced a rotameric switch of the Glu173 side chain, thus resulting in the disruption of two primary lumenal intermolecular hydrogen bonds (between the carboxyl oxygen of Glu173 and the backbone amide nitrogen of Ile74, with distances of 2.8 Å). Thus, only weak hydrogen-bond interactions (distances of 3.4 and 3.5 Å) at the lumenal side of DCCD-modified PsbS dimer were preserved in the structure (**Figs. 4d** and **7c**). We also compared the solution behavior of native and DCCD-modified PsbS at acidic pH through gel-filtration assays. The results revealed that the DCCD-modified PsbS eluted earlier than native PsbS at pH 5.0 (**Fig. 7d**) and resembled the form observed under neutral pH conditions (**Fig. 6a**). These results suggested that DCCD binding led to the disruption of intermolecular hydrogen bonds as well as to the relatively looser conformation of PsbS dimer.

DISCUSSION

Here we reported the long-awaited crystal structure of PsbS, an essential player in qE-type photoprotective energy dissipation in plants[15,17]. Our experimental data suggested that the low-pH crystal structure of the PsbS dimer represented the active state *in vivo*. Moreover, the cross-linking results of both dark-adapted thylakoids and the inactive E122Q E226Q double mutant of PsbS supported the previous report that the inactive PsbS is also dimeric[28]. Thus, the activation of PsbS by low pH probably involves a conformational change in PsbS while its dimeric form is maintained. Under neutral pH conditions, the two pH-sensing residues Glu69 and Glu173 would be deprotonated, thus causing the alteration of their hydrogen-bond interactions. The crystal structure of DCCD-modified PsbS showed that binding of DCCD disrupted the intermolecular hydrogen bonds mediated by Glu173 at the lumenal side. It has been reported that DCCD binds to *Arabidopsis* PsbS by targeting its two lumen-exposed glutamates[27], thus suggesting that DCCD can bind to Glu69 of spinach PsbS in addition to Glu173. However, we did not find electron density corresponding to DCNU in the vicinity of Glu69 in the DCCD-modified PsbS structure. The reason may be that in the crystal structure, Glu69 was located in a hydrophilic environment (**Fig. 7b**), and DCNU formation needs a hydrophobic environment[49,50]. Considering that the DCCD-modified PsbS structure was obtained from native PsbS crystal soaked in DCCD-containing solution, and hence it might not fully represent the structure of DCCD-modified PsbS in the thylakoid membranes, we presumed that when PsbS is embedded in the thylakoid membranes and surrounded by lipids and other membrane proteins (for example, LHCs), the side chain of Glu69 may switch its rotamer (similar to Glu173) to relocate into a relatively hydrophobic environment, and DCCD may also bind to Glu69 in a similar manner as that of Glu173, thus leading to the conformational change around the two lumenal loop regions. In addition, both DCCD-modified PsbS and the native PsbS at neutral pH adopted a dimeric conformation with weaker association at the lumenal side; this conformation might represent the inactive state of PsbS dimer *in vivo*. It is noteworthy that the PsbS dimer was unstable and tended to precipitate under neutral pH conditions, whereas it was very stable at low pH, thus suggesting that the PsbS dimer in its inactive form was flexible in the detergent solution. We propose that such a flexible PsbS dimer should be stabilized to a specific conformation when embedded in the thylakoid membranes with the native lipid environment. It is likely that the inactive PsbS dimer undergoes a limited conformational change at the lumenal side in the thylakoid membranes when activated by low pH, a process involving the alteration of the lumenal intermolecular hydrogen bonds within the PsbS dimer.

Regarding the intriguing pigment-binding properties of PsbS that are still under debate[21–26], our structural analysis revealed that PsbS adopts a unique folding pattern and cannot bind pigments (both chlorophylls and carotenoids) through the mode harnessed by other LHCs. The presence of chlorophyll in the PsbS protein and crystals might result from nonspecific association through hydrophobic interactions. However, considering that PsbS had a preference for binding Chl *a* over Chl *b* and that the stoichiometry of chlorophyll per PsbS dimer was approximately 1.0, an alternative possibility is that Chl *a* could associate with PsbS at the dimerization interface in an indirect manner mediated by water molecules (instead of being directly ligated to amino acid residues). The observation of this chlorophyll at the dimerization interface of PsbS suggests that PsbS may have a role in qE if this chlorophyll forms close interactions with other chlorophylls (from adjacent LHCs) or a zeaxanthin molecule under *in vivo* conditions[24].

In conclusion, our structural and biochemical analyses provide molecular insights into the mechanism of PsbS activation and inhibition. Nevertheless, how the activated PsbS initiates qE remains to be elucidated. It has been reported that under high-light conditions, PsbS originally associated with the PSII core migrates toward LHCs[28]. If the activated dimeric PsbS protein were inserted among the antennae, without internal pigment molecules to relay the excitation energy transfer, it might serve as an attenuator to dramatically slow down the energy flow among the LHCs. In addition, the activated PsbS dimer may interact directly with neighboring LHCs, promote their conformational changes and induce quenching within the LHCs or at their interfacial area. The direct interaction between PsbS and an LHC during qE is supported by previous pulldown assays[51] and by the recent successful *in vitro* reconstitution of the quenching process with a proteoliposome system containing PsbS, LHCII and zeaxanthin[42]. It is also possible that PsbS may participate in qE indirectly by acting solely as a pH-sensing trigger or as a catalyst. Recent studies have shown that qE formation is correlated with a structural reorganization of the PSII–LHCII supercomplex in the thylakoid membranes and have suggested that PsbS controls this reorganization[8,52–57], which could be transduced by the low pH–induced conformational change of the PsbS dimer. The PsbS structures presented here should serve as a foundation for further exploration on the mechanism of PsbS function in qE.

METHODS

Methods and any associated references are available in the online version of the paper.

Accession codes. Coordinates and structure factors for PsbS and DCCD-modified PsbS have been deposited in the Protein Data Bank under accession codes 4RI2 and 4RI3, respectively.

Note: Any Supplementary Information and Source Data files are available in the online version of the paper.

ACKNOWLEDGMENTS

We thank R. Bassi (Dipartimento di Biotecnologie, Università di Verona) for discussion, manuscript reading and providing seeds of *npq4*-E122Q E226Q double-mutant *Arabidopsis*, and N. Isaacs, K.K. Niyogi and J. Barber for manuscript reading. We are grateful to the staff at the Shanghai Synchrotron Radiation Facility and the Photo Factory for technical support. This work was supported by grants 2011CBA00902 (to W.C.) and 2011CBA00903 (to Z.L.) from the National Key Basic Research Program of China; grant XDB08020302 (to W.C.) from the Strategic Priority Research Program of the Chinese Academy of Sciences; and grants 31021062 (to W.C.), 31270793 (to M.L.), 31170703 (to X.P.), and 31100534 (to P.C.) from the National Natural Science Foundation of China.

AUTHOR CONTRIBUTIONS

M.F., M.L. and W.C. conceived the project. M.F. purified PsbS and performed the structural determination and the biochemical experiments with PsbS.

P.C., M.L. and H.Z. assisted with data collection. X.Z. and J.Z. assisted with isolation of BBY membranes. X.P. assisted with HPLC experiments. M.F., M.L., Z.L. and W.C. discussed the results and wrote the manuscript.

COMPETING FINANCIAL INTERESTS

The authors declare no competing financial interests.

1. Caffarri, S., Kouřil, R., Kereïche, S., Boekema, E.J. & Croce, R. Functional architecture of higher plant photosystem II supercomplexes. *EMBO J.* **28**, 3052–3063 (2009).
2. Demmig-Adams, B. & Adams, W.W. III. Photoprotection and other responses of plants to high light stress. *Annu. Rev. Plant Physiol. Plant Mol. Biol.* **43**, 599–626 (1992).
3. Apel, K. & Hirt, H. Reactive oxygen species: metabolism, oxidative stress, and signal transduction. *Annu. Rev. Plant Biol.* **55**, 373–399 (2004).
4. Horton, P., Ruban, A.V. & Walters, R.G. Regulation of light harvesting in green plants. *Annu. Rev. Plant Physiol. Plant Mol. Biol.* **47**, 655–684 (1996).
5. Müller, P., Li, X.-P. & Niyogi, K.K. Non-photochemical quenching: a response to excess light energy. *Plant Physiol.* **125**, 1558–1566 (2001).
6. de Bianchi, S., Ballottari, M., Dall'osto, L. & Bassi, R. Regulation of plant light harvesting by thermal dissipation of excess energy. *Biochem. Soc. Trans.* **38**, 651–660 (2010).
7. Külheim, C., Ågren, J. & Jansson, S. Rapid regulation of light harvesting and plant fitness in the field. *Science* **297**, 91–93 (2002).
8. Ruban, A.V., Johnson, M.P. & Duffy, C.D.P. The photoprotective molecular switch in the photosystem II antenna. *Biochim. Biophys. Acta* **1817**, 167–181 (2012).
9. Rochaix, J.D. Regulation and dynamics of the light-harvesting system. *Annu. Rev. Plant Biol.* **65**, 287–309 (2014).
10. Kramer, D.M., Sacksteder, C.A. & Cruz, J.A. How acidic is the lumen? *Photosynth. Res.* **60**, 151–163 (1999).
11. Demmig-Adams, B. Carotenoids and photoprotection in plants: a role for the xanthophyll zeaxanthin. *Biochim. Biophys. Acta* **1020**, 1–24 (1990).
12. Ruban, A.V. *et al.* Identification of a mechanism of photoprotective energy dissipation in higher plants. *Nature* **450**, 575–578 (2007).
13. Ahn, T.K. *et al.* Architecture of a charge-transfer state regulating light harvesting in a plant antenna protein. *Science* **320**, 794–797 (2008).
14. Bode, S. *et al.* On the regulation of photosynthesis by excitonic interactions between carotenoids and chlorophylls. *Proc. Natl. Acad. Sci. USA* **106**, 12311–12316 (2009).
15. Li, X.-P. *et al.* A pigment-binding protein essential for regulation of photosynthetic light harvesting. *Nature* **403**, 391–395 (2000).
16. Kasajima, I. *et al.* Molecular distinction in genetic regulation of nonphotochemical quenching in rice. *Proc. Natl. Acad. Sci. USA* **108**, 13835–13840 (2011).
17. Brooks, M.D., Jansson, S. & Niyogi, K.K. in *Non-Photochemical Quenching and Energy Dissipation in Plants, Algae and Cyanobacteria* Vol. 40 (eds. Demmig-Adams, B., Garab, G., Adams, W.W. III & Govindjee, U.o.I.) 297–314 (Springer, 2014).
18. Li, X.-P., Gilmore, A.M. & Niyogi, K.K. Molecular and global time-resolved analysis of a *psbS* gene dosage effect on pH- and xanthophyll cycle-dependent nonphotochemical quenching in photosystem II. *J. Biol. Chem.* **277**, 33590–33597 (2002).
19. Li, X.-P., Müller-Moulé, P., Gilmore, A.M. & Niyogi, K.K. PsbS-dependent enhancement of feedback de-excitation protects photosystem II from photoinhibition. *Proc. Natl. Acad. Sci. USA* **99**, 15222–15227 (2002).
20. Barros, T. & Kühlbrandt, W. Crystallisation, structure and function of plant light-harvesting complex II. *Biochim. Biophys. Acta* **1787**, 753–772 (2009).
21. Funk, C., Schroder, W.P., Green, B.R., Renger, G. & Andersson, B. The intrinsic 22 kDa protein is a chlorophyll-binding subunit of photosystem II. *FEBS Lett.* **342**, 261–266 (1994).
22. Funk, C. *et al.* The PSII-S protein of higher plants: a new type of pigment-binding protein. *Biochemistry* **34**, 11133–11141 (1995).
23. Aspinall-O'Dea, M. *et al. In vitro* reconstitution of the activated zeaxanthin state associated with energy dissipation in plants. *Proc. Natl. Acad. Sci. USA* **99**, 16331–16335 (2002).
24. Niyogi, K.K., Li, X.-P., Rosenberg, V. & Jung, H.S. Is PsbS the site of non-photochemical quenching in photosynthesis? *J. Exp. Bot.* **56**, 375–382 (2005).
25. Dominici, P. *et al.* Biochemical properties of the PsbS subunit of photosystem II either purified from chloroplast or recombinant. *J. Biol. Chem.* **277**, 22750–22758 (2002).
26. Bonente, G., Howes, B.D., Caffarri, S., Smulevich, G. & Bassi, R. Interactions between the photosystem II subunit PsbS and xanthophylls studied *in vivo* and *in vitro*. *J. Biol. Chem.* **283**, 8434–8445 (2008).
27. Li, X.-P. *et al.* Regulation of photosynthetic light harvesting involves intrathylakoid lumen pH sensing by the PsbS protein. *J. Biol. Chem.* **279**, 22866–22874 (2004).
28. Bergantino, E. *et al.* Light- and pH-dependent structural changes in the PsbS subunit of photosystem II. *Proc. Natl. Acad. Sci. USA* **100**, 15265–15270 (2003).
29. Johnson, M.P. & Ruban, A.V. *Arabidopsis* plants lacking PsbS protein possess photoprotective energy dissipation. *Plant J.* **61**, 283–289 (2010).
30. Johnson, M.P. & Ruban, A.V. Restoration of rapidly reversible photoprotective energy dissipation in the absence of PsbS protein by enhanced ΔpH. *J. Biol. Chem.* **286**, 19973–19981 (2011).
31. Horton, P. *et al. PS2001 Proc. 12th International Congress on Photosynthesis* PL-003 (CSIRO Publishing, Melbourne, Australia, 2001).
32. Li, X.-P., Phippard, A., Pasari, J. & Niyogi, K.K. Structure-function analysis of photosystem II subunit S (PsbS) *in vivo*. *Funct. Plant Biol.* **29**, 1131–1139 (2002).
33. Schultes, N.P. & Peterson, R.B. Phylogeny-directed structural analysis of the *Arabidopsis* PsbS protein. *Biochem. Biophys. Res. Commun.* **355**, 464–470 (2007).
34. Wedel, N., Klein, R., Ljungberg, U., Andersson, B. & Herrmann, R.G. The single-copy gene psbS codes for a phylogenetically intriguing 22 kDa polypeptide of photosystem II. *FEBS Lett.* **314**, 61–66 (1992).
35. Kim, S. *et al.* Characterization of a spinach psbS cDNA encoding the 22 kDa protein of photosystem II. *FEBS Lett.* **314**, 67–71 (1992).
36. Jansson, S. A guide to the *Lhc* genes and their relatives in *Arabidopsis*. *Trends Plant Sci.* **4**, 236–240 (1999).
37. Liu, Z. *et al.* Crystal structure of spinach major light-harvesting complex at 2.72 Å resolution. *Nature* **428**, 287–292 (2004).
38. Pan, X. *et al.* Structural insights into energy regulation of light-harvesting complex CP29 from spinach. *Nat. Struct. Mol. Biol.* **18**, 309–315 (2011).
39. Amunts, A., Toporik, H., Borovikova, A. & Nelson, N. Structure determination and improved model of plant photosystem I. *J. Biol. Chem.* **285**, 3478–3486 (2010).
40. Pan, X., Liu, Z.F., Li, M. & Chang, W.R. Architecture and function of plant light-harvesting complexes II. *Curr. Opin. Struct. Biol.* **23**, 515–525 (2013).
41. Funk, C., Adamska, I., Green, B.R., Andersson, B. & Renger, G. The nuclear-encoded chlorophyll-binding photosystem II-S protein is stable in the absence of pigments. *J. Biol. Chem.* **270**, 30141–30147 (1995).
42. Wilk, L., Grunwald, M., Liao, P.N., Walla, P.J. & Kühlbrandt, W. Direct interaction of the major light-harvesting complex II and PsbS in nonphotochemical quenching. *Proc. Natl. Acad. Sci. USA* **110**, 5452–5456 (2013).
43. Plumley, F.G. & Schmidt, G.W. Reconstitution of chlorophyll a/b light-harvesting complexes: xanthophyll-dependent assembly and energy transfer. *Proc. Natl. Acad. Sci. USA* **84**, 146–150 (1987).
44. Magalhaes, A., Maigret, B., Hoflack, J., Gomes, J.A.N.F. & Scheraga, H.A. Contribution of unusual arginine-arginine short-range interactions to stabilization and recognition in proteins. *J. Protein Chem.* **13**, 195–215 (1994).
45. Krissinel, E. & Henrick, K. Inference of macromolecular assemblies form crystalline state. *J. Mol. Biol.* **372**, 774–797 (2007).
46. Goss, R., Opitz, C., Lepetit, B. & Wilhelm, C. The synthesis of NPQ-effective zeaxanthin depends on the presence of a transmembrane proton gradient and a slightly basic stromal side of the thylakoid membrane. *Planta* **228**, 999–1009 (2008).
47. Zaks, J., Amarnath, K., Sylak-Glassman, E.J. & Fleming, G.R. Models and measurements of energy-dependent quenching. *Photosynth. Res.* **116**, 389–409 (2013).
48. Azzi, A., Casey, R.P. & Nalecz, M.J. The effect of *N,N′*-dicyclohexylcarbodiimide on enzymes of bioenergetic relevance. *Biochim. Biophys. Acta* **768**, 209–226 (1984).
49. Mizutani, K. *et al.* Structure of the rotor ring modified with *N,N′*-dicyclohexylcarbodiimide of the Na^+-transporting vacuolar ATPase. *Proc. Natl. Acad. Sci. USA* **108**, 13474–13479 (2011).
50. Pogoryelov, D. *et al.* Microscopic rotary mechanism of ion translocation in the F_O complex of ATP synthases. *Nat. Chem. Biol.* **6**, 891–899 (2010).
51. Teardo, E. *et al.* Evidences for interaction of PsbS with photosynthetic complexes in maize thylakoids. *Biochim. Biophys. Acta* **1767**, 703–711 (2007).
52. Johnson, M.P. *et al.* Photoprotective energy dissipation involves the reorganization of photosystem II light-harvesting complexes in the grana membranes of spinach chloroplasts. *Plant Cell* **23**, 1468–1479 (2011).
53. Betterle, N. *et al.* Light-induced dissociation of an antenna hetero-oligomer is needed for non-photochemical quenching induction. *J. Biol. Chem.* **284**, 15255–15266 (2009).
54. Kiss, A.Z., Ruban, A.V. & Horton, P. The PsbS protein controls the organization of the photosystem II antenna in higher plant thylakoid membranes. *J. Biol. Chem.* **283**, 3972–3978 (2008).
55. Kereïche, S., Kiss, A.Z., Kouril, R., Boekema, E.J. & Horton, P. The PsbS protein controls the macro-organisation of photosystem II complexes in the grana membranes of higher plant chloroplasts. *FEBS Lett.* **584**, 759–764 (2010).
56. Goral, T.K. *et al.* Light-harvesting antenna composition controls the macrostructure and dynamics of thylakoid membranes in *Arabidopsis*. *Plant J.* **69**, 289–301 (2012).
57. Sylak-Glassman, E.J. *et al.* Distinct roles of the photosystem II protein PsbS and zeaxanthin in the regulation of light harvesting in plants revealed by fluorescence lifetime snapshots. *Proc. Natl. Acad. Sci. USA* **111**, 17498–17503 (2014).

ONLINE METHODS

Protein purification. BBY membranes were prepared from fresh market spinach as previously described[58]. PsbS was selectively precipitated from the BBY membranes as reported[59]. Briefly, the BBY membranes were suspended with a buffer containing 20 mM MES, pH 6.0, 15 mM NaCl, and 0.4 M sucrose at a chlorophyll concentration of 0.5 mg ml^{-1} and then solubilized with 0.4% *n*-octyl-β-D-thioglucopyranoside (OTG, Anatrace) on ice for 10 min. After solubilization, the sample was centrifuged at 40,000*g* for 40 min to obtain the PsbS-enriched precipitate. The precipitate was suspended with a buffer containing 20 mM sodium acetate, pH 5.0, and 20 mM NaCl (buffer A). PsbS was subsequently solubilized by 2% *n*-octyl-β-D-glucopyranoside (OG, Anatrace) with overnight incubation at 4 °C. Solubilized PsbS was separated from the insoluble fraction by centrifugation at 40,000*g* for 30 min. The supernatant was applied to a Resource S column (GE Healthcare) preequilibrated with buffer A supplemented with 0.4% *n*-nonyl-β-D-glucopyranoside (NG, Anatrace). The bound PsbS protein was then eluted by NaCl gradient and incubated with subtilisin (Hampton Research) at 20 °C for 2 h, with a final concentration of 0.01 mg ml^{-1} subtilisin. After limited proteolysis, the resultant PsbS protein was applied to a Superdex 200 column (GE Healthcare) preequilibrated with a buffer containing 20 mM sodium acetate, pH 5.0, 100 mM NaCl, and 0.4% NG. The peak fraction containing PsbS was collected and concentrated to 10 mg ml^{-1}. N-terminal sequence analysis revealed that the first five residues of PsbS, i.e., LFKSK, were removed by the subtilisin treatment.

Crystallization. The PsbS crystals were grown at 20 °C by the sitting-drop vapor-diffusion method. The protein was mixed with an equal volume of a reservoir solution containing 100 mM sodium acetate, pH 5.0, 25–28% PEG 300 and 1% ethyl acetate. Crystals of maximal sizes were obtained after 10 d. The heavy atom–derivative crystals were obtained by soaking in the presence of 10 mM mercury nitrate for 1 d. The DCCD-modified PsbS crystals were obtained by soaking in the presence of 10 mM *N*,*N*′-dicyclohexylcarbodiimide (DCCD, Sigma) for 3 d. For data collection, the reservoir solution supplemented with 0.5% NG and 18% glycerol was used as cryoprotectant solution during crystal manipulation, and the crystals were rapidly frozen in liquid nitrogen.

Data collection and structure determination. We collected two sets of diffraction data for native PsbS crystals, naming the low-resolution data (3.1 Å) native 1 and the higher resolution data (2.35 Å) native 2. The diffraction data of both native 1 and heavy atom–derivative crystals were collected at 100 K with an ADSC Q315 CCD detector at beamline BL17U of the Shanghai Synchrotron Radiation Facility. The diffraction data of both native 2 and DCCD-bound PsbS crystals were collected at beamline NE3A of the Photon Factory. The data were indexed, integrated and scaled with HKL2000 (ref. 60). Further structure determination and refinement were performed with PHENIX[61].

Because initial molecular replacement with PHASER[62] and search models derived from LHCII and CP29 didn't give a reasonable solution, mercury derivatives were prepared for phasing. We determined the structure with the diffraction data of native 1 and mercury-derivative crystals through the single isomorphous replacement with anomalous scattering (SIRAS) method. Five mercury sites were identified with SHELX[63], and the phase was calculated by PHENIX AutoSol. An initial model at 3.1-Å resolution was obtained by a combination of PHENIX AutoBuild and manual building with Coot[64], and the resolution was finally extended to 2.35 Å. The structure of DCCD-modified PsbS was solved by molecular replacement with the native PsbS structure as the search model and was refined to 2.7 Å with phenix.refine. Data collection and refinement statistics are presented in **Table 1**.

The stereochemical quality of the refined structures was verified with PROCHECK[65]. The Ramachandran statistics for the structures of PsbS and DCCD-modified PsbS are 95.2% favored, 4.8% allowed, 0% outliers; and 95.1% favored, 4.9% allowed, 0% outliers, respectively. All structural representations in this paper were prepared with PyMOL (http://www.pymol.org/). Considering that the N-terminal part (residues 6–16) of molecule A of the PsbS structure has a weak electron density, and the counterpart of molecule B is unseen, owing to presumable flexibility in the PsbS dimer, we have not included residues 6–16 of molecule A in all structural representations.

Gel-filtration assay. A Superdex 200 column was used for gel-filtration assays. For analyzing the oligomeric state of PsbS at pH 5.0, its molecular weight was estimated with two LHC proteins with known molecular weights (LHCII, 122 kDa; CP29, 42 kDa) as standards. The column was preequilibrated with a buffer containing 20 mM sodium acetate, pH 5.0, 100 mM NaCl, and 0.4% NG (buffer B). PsbS, CP29 and LHCII were injected into the column and eluted at a flow rate of 0.4 ml min^{-1}. For comparison of the solution behaviors of PsbS at low and neutral pH, the column was preequilibrated with a buffer containing 20 mM sodium acetate, pH 5.0, 200 mM NaCl, 50 mM $MgCl_2$, and 0.4% NG, or a buffer containing 20 mM HEPES, pH 7.3, 200 mM NaCl, 50 mM $MgCl_2$, and 0.4% NG. PsbS was injected onto the column and eluted at a flow rate of 0.4 ml min^{-1}. For comparison of the solution behaviors of PsbS and DCCD-modified PsbS, the column was preequilibrated with buffer B. DCCD-modified PsbS was obtained by incubation of native PsbS with DCCD in buffer B at 20 °C for 30 min, with a final concentration of 10 mM for DCCD. PsbS and DCCD-modified PsbS were injected onto the column and eluted at a flow rate of 0.4 ml min^{-1}.

Chemical cross-linking. For cross-linking of purified PsbS at low pH, PsbS was incubated with 1-ethyl-3-(3-dimethylaminopropyl) carbodiimide (EDC, Sigma) in a buffer containing 50 mM NaH_2PO_4, pH 5.0, 4.0, or 3.0, 150 mM NaCl, and 0.4% NG at 20 °C for 1 h, with a final concentration of 1 mg ml^{-1} PsbS and different concentrations of EDC. The reaction was stopped by addition of an equal volume of 2× SDS-PAGE loading buffer, and the reaction products were analyzed by SDS-PAGE. For cross-linking in PsbS-containing thylakoids at pH 5.0, we prepared both low pH–incubated and high light–treated thylakoids from spinach, maize, and *Arabidopsis*. For preparation of low pH–incubated thylakoids, the thylakoids were suspended in a buffer containing 50 mM NaH_2PO_4, pH 5.0, 10 mM NaCl, 5 mM $MgCl_2$, and 100 mM sorbitol and were then incubated at 20 °C for 40 min. For preparation of high light–treated thylakoids, the thylakoids were diluted to a chlorophyll concentration of 20 μg ml^{-1} in a buffer containing 20 mM HEPES, pH 7.5, 10 mM NaCl, 5 mM $MgCl_2$, and 100 mM sorbitol, and then illuminated with 600 μmol photons m^{-2} s^{-1} for 20 min. The treated thylakoids were collected and incubated with EDC in a buffer containing 50 mM NaH_2PO_4, pH 5.0, 10 mM NaCl, 5 mM $MgCl_2$, 100 mM sorbitol, and 1% *n*-dodecyl-β-D-maltopyranoside (DDM, Anatrace) at 20 °C for 2–4 h, with a final concentration of 0.8 mg ml^{-1} for chlorophyll and a final concentration of 20 mM for EDC. The reaction was stopped by addition of an equal volume of 2× SDS-PAGE loading buffer, and the reaction products were analyzed by SDS-PAGE. The proteins were then transferred to a PVDF membrane and probed with anti-PsbS polyclonal antibody (Agrisera, cat. no. AS09 533). The validation of reactivities of this antibody with PsbS from *Arabidopsis*, spinach and maize is provided on the manufacturer's website. For cross-linking in PsbS-containing chloroplasts at pH 5.0, we prepared intact chloroplasts from spinach leaves, following a previously described protocol[66]. To prepare high light–treated chloroplasts, the chloroplasts were diluted to a chlorophyll concentration of 20 μg ml^{-1} in a buffer containing 20 mM HEPES, pH 7.6, 330 mM sorbitol, 2 mM EDTA, 1 mM $MgCl_2$, 1 mM $MnCl_2$, 1 mM NaCl, and 10 mM KCl, and then illuminated with 600 μmol photons m^{-2} s^{-1} for 30 min. The subsequent procedures are similar to the above-described procedures for cross-linking in thylakoids. For cross-linking in PsbS-containing dark-adapted thylakoids at neutral pH, the thylakoids were incubated with ethylene glycol bis(sulfosuccinimidyl succinate) (Sulfo-EGS, Thermo Scientific Pierce) or bis(succinimidyl) penta(ethylene glycol) ($BS(PEG)_5$, Thermo Scientific Pierce) in a buffer containing 50 mM HEPES, pH 7.5, 150 mM NaCl, and 1% DDM at 20 °C for 30 min, with a final concentration of 0.9 mg ml^{-1} chlorophyll and final concentrations of 0, 0.1 mM, 0.2 mM, 0.5 mM and 1.0 mM for Sulfo-EGS or $BS(PEG)_5$. The reaction was stopped by addition of an equal volume of 2× SDS-PAGE loading buffer, and the reaction products were analyzed by SDS-PAGE. The proteins were then transferred to a PVDF membrane and probed with anti-PsbS polyclonal antibody. Original images of gels and blots used in this study can be found in **Supplementary Data Set 1**.

Pigment analysis. Pigments were extracted with 80% (v/v) acetone and analyzed by high-performance liquid chromatography, as previously described[67]. Individual pigments were identified by the absorption spectrum of each peak.

Spectroscopy. The absorption and CD spectra of purified PsbS protein in buffer B at 20 °C were recorded with a Hitachi U3010 spectrophotometer

doi:10.1038/nsmb.3068

and Chirascan Plus spectrometer (Applied Photophysics), respectively. Chl *a* (Sigma) and purified LHCII protein were used as controls for absorption and CD measurements, respectively.

Mass spectrometry. The molecular weights of native PsbS and DCCD-incubated PsbS were determined with quadrupole time-of-flight mass spectrometer.

58. Berthold, D.A., Babcock, G.T. & Yocum, C.F. A highly resolved, oxygen-evolving photosystem II preparation from spinach thylakoid membranes. *FEBS Lett.* **134**, 231–234 (1981).
59. Mishra, R.K. & Ghanotakis, D.F. Selective extraction of CP26 and CP29 proteins without affecting the binding of the extrinsic protein (33, 23 and 17 kDa) and the DCMU sensitivity of a photosystem II core complex. *Photosynth. Res.* **42**, 37–42 (1994).
60. Otwinowski, Z. & Minor, W. Processing of X-ray diffraction data collected in oscillation mode. *Methods Enzymol.* **276**, 307–326 (1997).
61. Adams, P.D. *et al. PHENIX*: a comprehensive Python-based system for macromolecular structure solution. *Acta Crystallogr. D Biol. Crystallogr.* **66**, 213–221 (2010).
62. McCoy, A.J. *et al. Phaser* crystallographic software. *J. Appl. Crystallogr.* **40**, 658–674 (2007).
63. Sheldrick, G.M. A short history of *SHELX*. *Acta Crystallogr. A* **64**, 112–122 (2008).
64. Emsley, P. & Cowtan, K. *Coot*: model-building tools for molecular graphics. *Acta Crystallogr. D Biol. Crystallogr.* **60**, 2126–2132 (2004).
65. Laskowski, R.A., Macarthur, M.W., Moss, D.S. & Thornton, J.M. *PROCHECK*: a program to check the stereochemical quality of protein structures. *J. Appl. Crystallogr.* **26**, 283–291 (1993).
66. Joly, D. & Carpentier, R. in *Photosynthesis Research Protocols, Methods in Molecular Biology* Vol. 684 (ed. Carpentier, R.) 321–325 (Springer, 2011).
67. Farber, A., Young, A.J., Ruban, A.V., Horton, P. & Jahns, P. Dynamics of xanthophyll-cycle activity in different antenna subcomplexes in the photosynthetic membranes of higher plants: the relationship between zeaxanthin conversion and nonphotochemical fluorescence quenching. *Plant Physiol.* **115**, 1609–1618 (1997).